

Fig. S1. Blimp-1 expression in the retina. Blimp-1 antibody staining (A''', B''', C''', red in A-C) in a third-instar larval eye disc (A) with *Blimp-1*¹⁷ clones marked with GFP (A', green in A), a 46 h APF pupal retina with *Blimp-1*¹⁷ clones marked with GFP (B', green in B, outlined in B''') and a 72 h APF wild type pupal retina (C). Other antibodies used are Elav (A'', C', blue in A, green in C) and Cut (B'', C'', blue in B, C). Panels in (B) are confocal sections taken from the same retina as Fig. 1L at the level of photoreceptor and primary pigment cell nuclei. Scale bars, 50 μ m (A), 20 μ m (B, C).

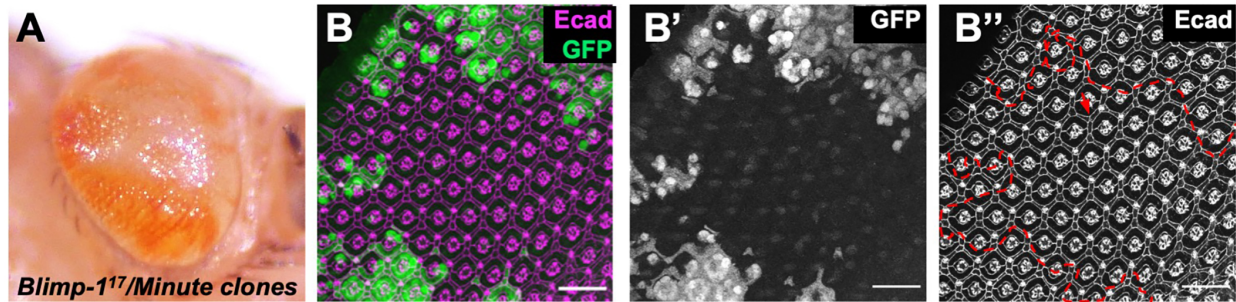


Fig. S2. Blimp-1 is not required for cell fate determination in the eye. (A) Adult eye containing large *Blimp-1*¹⁷ mutant clones (white) generated in a *Minute* background. (B) 42 h APF pupal retina containing large *Blimp-1*¹⁷ mutant clones generated in a *Minute* background (outlined), marked by the absence of GFP (B', green in B) and stained for Ecad (B'', magenta in B). The ommatidial array appears largely normal in the *Blimp-1* mutant region (arrow in B'' indicates a missing tertiary pigment cell, observed in approximately 5% of ommatidia). Scale bar, 20 μ m.

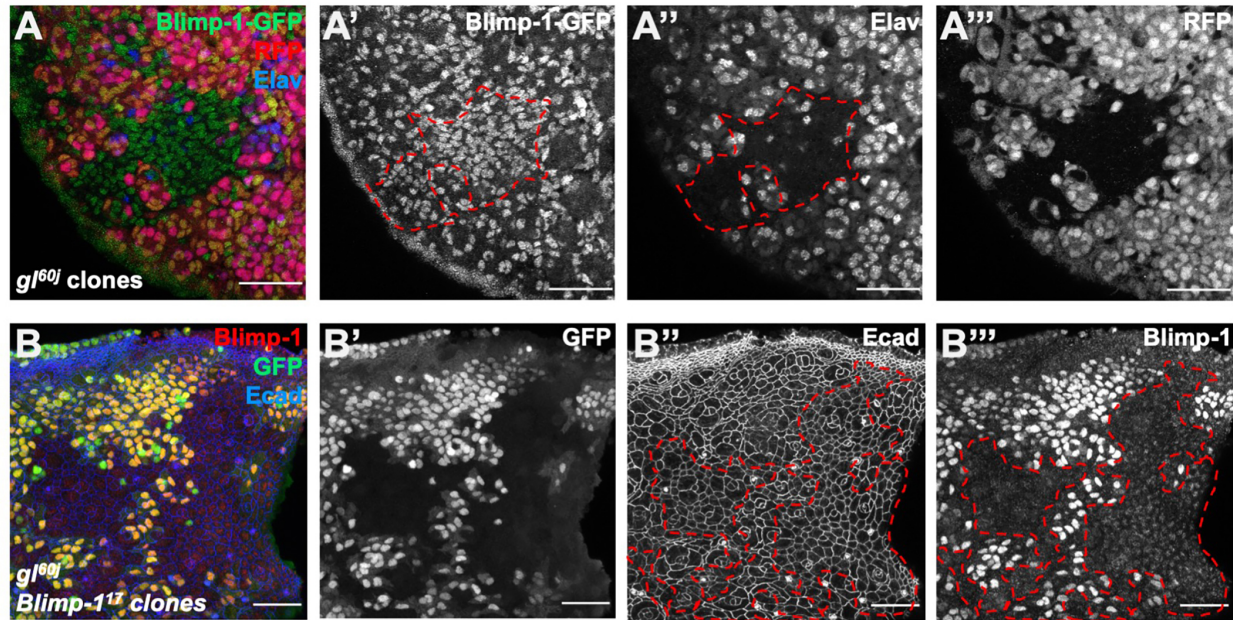


Fig. S3. Gl inhibits *Blimp-1* expression in the retina. (A) 46 h APF pupal retina containing *gl*^{60j} mutant clones (outlined) marked by the absence of RFP (A''', red in A), stained with anti-GFP to reveal the Blimp-1 protein trap Blimp-1-GFP.FPTB (A', green in A) and anti-Elav (A'', blue in A). In the mutant region, an increased number of cells express Blimp-1, and these cells do not express the photoreceptor marker Elav. (B) 46 h APF *gl*^{60j} mutant retina in which *Blimp-1* mutant clones (outlined) are marked by the absence of GFP (B', green in B), stained for Ecad (B'', blue in B) and Blimp-1 (B''', red in B). The disorganized Ecad-marked lattice typical of *gl* mutant retinas is not rescued in the *Blimp-1* mutant regions. Scale bars, 20µm.

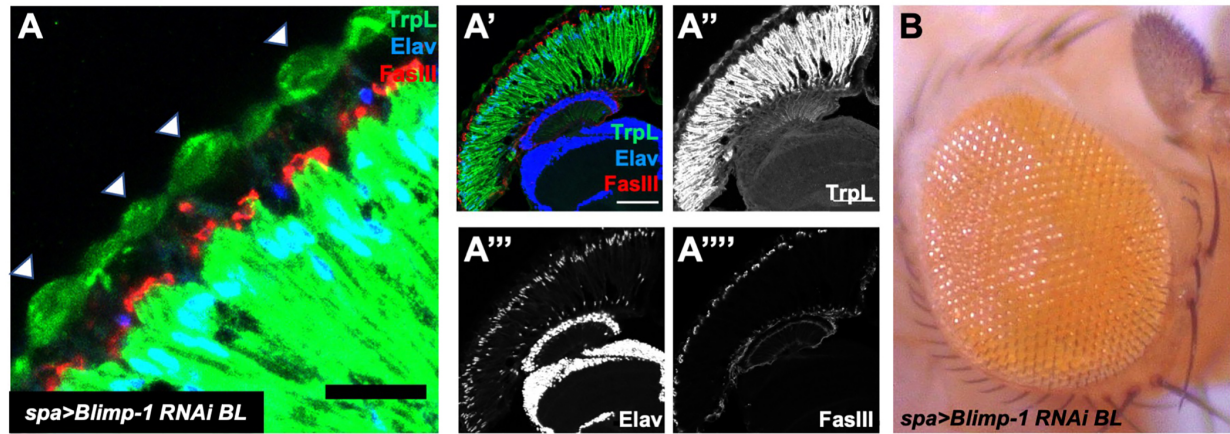


Fig. S4. Loss of Blimp-1 from cone and primary pigment cells does not alter corneal lens shape. (A) Horizontal section of adult head in which *Blimp-1* RNAi is driven in cone and primary pigment cells with *spa-GAL4*, stained for TrpL (A'', green), Elav (A''', blue) and Fasciclin III (FasIII), which marks the apical region of cone cells (A''', red). Arrowheads in (A) indicate bi-convex corneal lenses. Scale bars, 20 μ m (A) or 50 μ m (A'). (B) Adult eye with *Blimp-1* RNAi driven by *spa-GAL4*. Individual corneal lenses are visible, but the eye is slightly rough due to photoreceptor defects.

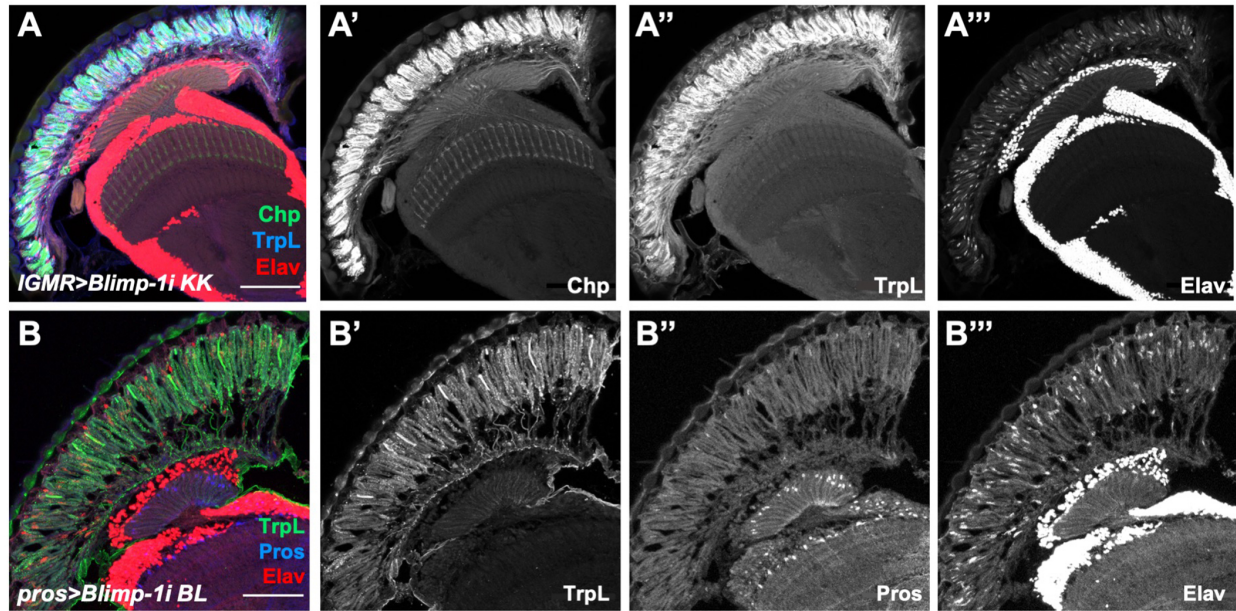


Fig. S5. Blimp-1 knockdown disrupts photoreceptor morphology. (A) Horizontal section of an adult head in which *Blimp-1* RNAi is driven by *IGMR-GAL4*, stained for Chp (A', green in A), TrpL (A'', blue in A) and Elav (A''', red in A). The photoreceptor rhabdomeres are short, reducing the thickness of the retina, and their nuclei are disorganized. (B) Horizontal section of an adult eye in which *Blimp-1* RNAi is expressed in cone cells with *pros-GAL4*, stained for TrpL (B', green), Pros (B'', blue) and Elav (B''', red). Rhabdomeres do not extend into the proximal region, and photoreceptor nuclei are disorganized. Scale bars, 50 μ m.

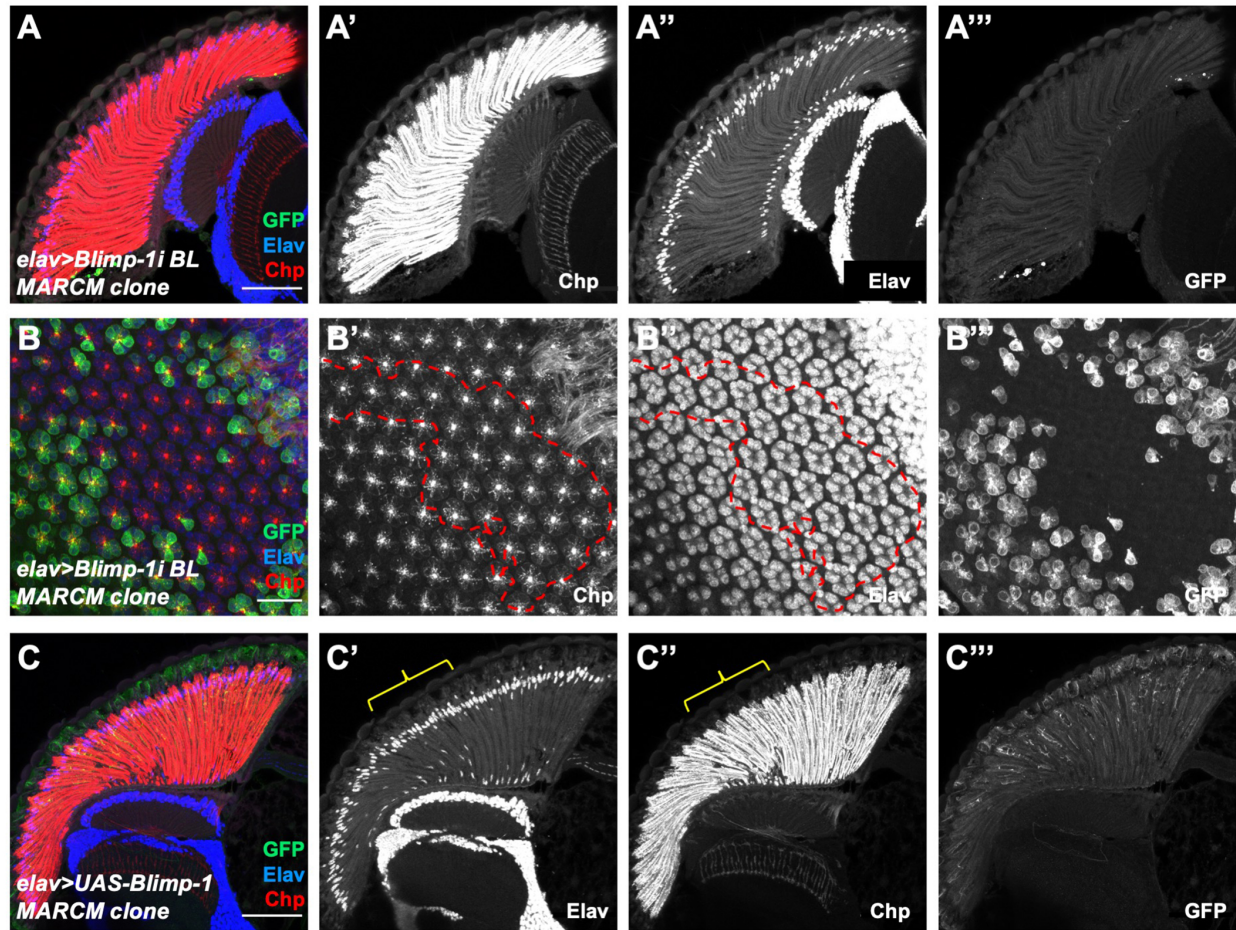


Fig. S6. Increasing, but not reducing, Blimp-1 in photoreceptors causes abnormal morphology.

(A, C) Horizontal sections of adult eyes or (B) 46 h APF pupal retina with clones expressing *Blimp-1* RNAi (A, B) or *UAS-Blimp-1*^{72.1} (C) in photoreceptors with *elav-GAL4*, stained for GFP to mark the clones (A'''-C''', green in A-C), Chp (A'-C', red in A-C) and Elav (A''-C'', blue in A-C). *elav-GAL4* is no longer expressed in the adult, but (B) shows that clones are present (outlined). Expressing *Blimp-1* RNAi causes no visible defects, but overexpressing Blimp-1 disrupts photoreceptor rhabdomeres and nuclei. The bracket in (C) marks a region of abnormal morphology that is likely to be an overexpression clone. Scale bars, 50 μ m (A, C) or 20 μ m (B).

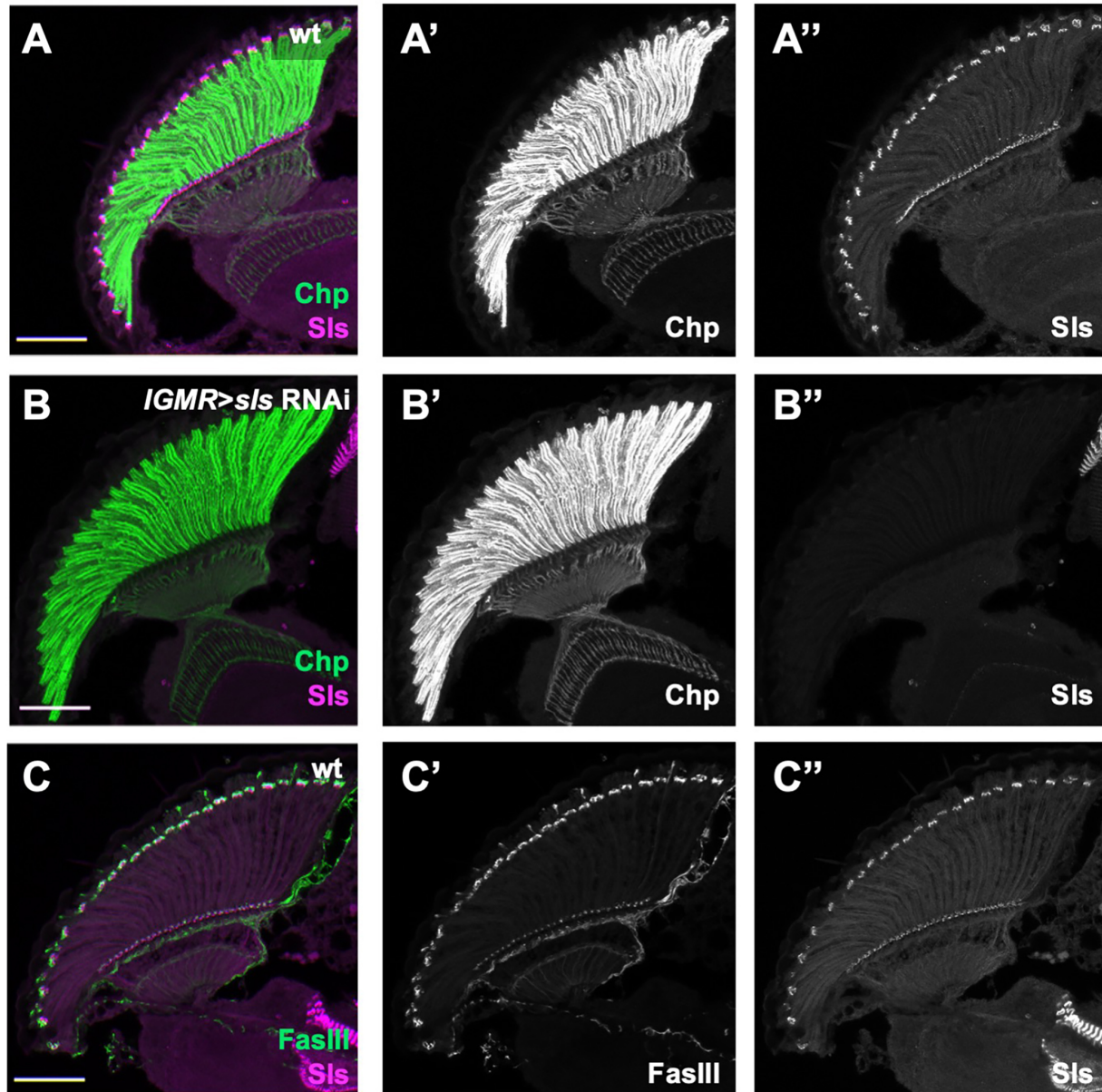


Fig. S7. Sls is expressed in cone cell feet. Cryostat sections of adult heads stained for Chp (A', B', green in A, B), Sls (A'', B'', C'', magenta in A-C) and FasIII (C', green in C). (A, C) wild type; (B) *IGMR-GAL4* driving *sls* RNAi. Sls is present in the apical regions of cone cells, where it colocalizes with FasIII, and in cone cell feet. The loss of both sites of Sls staining when *sls* RNAi is expressed throughout the eye confirms the antibody specificity. Scale bars, 50 μ m.

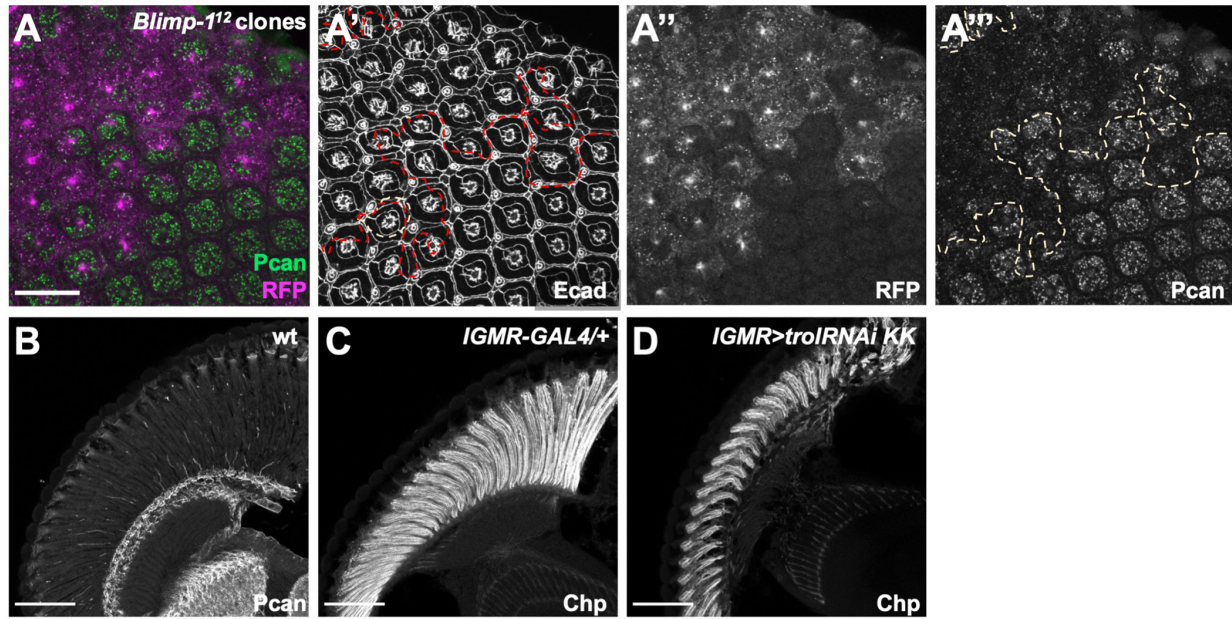


Fig. S8. *trol* is regulated by Blimp-1 in cone cells and required for rhabdomere extension. (A) 46 h APF retina with *Blimp-1*¹² clones marked by the absence of RFP (A'', magenta in A) and outlined with dashed lines, stained for Pcan (A''', green in A) and Ecad (A'). Pcan is present in the central cone cells in each ommatidium and its expression is strongly reduced in *Blimp-1* mutant regions. (B-D) Adult head sections stained for Pcan (B) or Chp (C, D). (B) wild type; (C) *IGMR-GAL4/+*; (D) *IGMR-GAL4* driving *trol* RNAi. Pcan is localized to cone cell feet, and knocking down *trol* results in shortened rhabdomeres. Scale bars, 20 μm (A) or 50 μm (B-D).

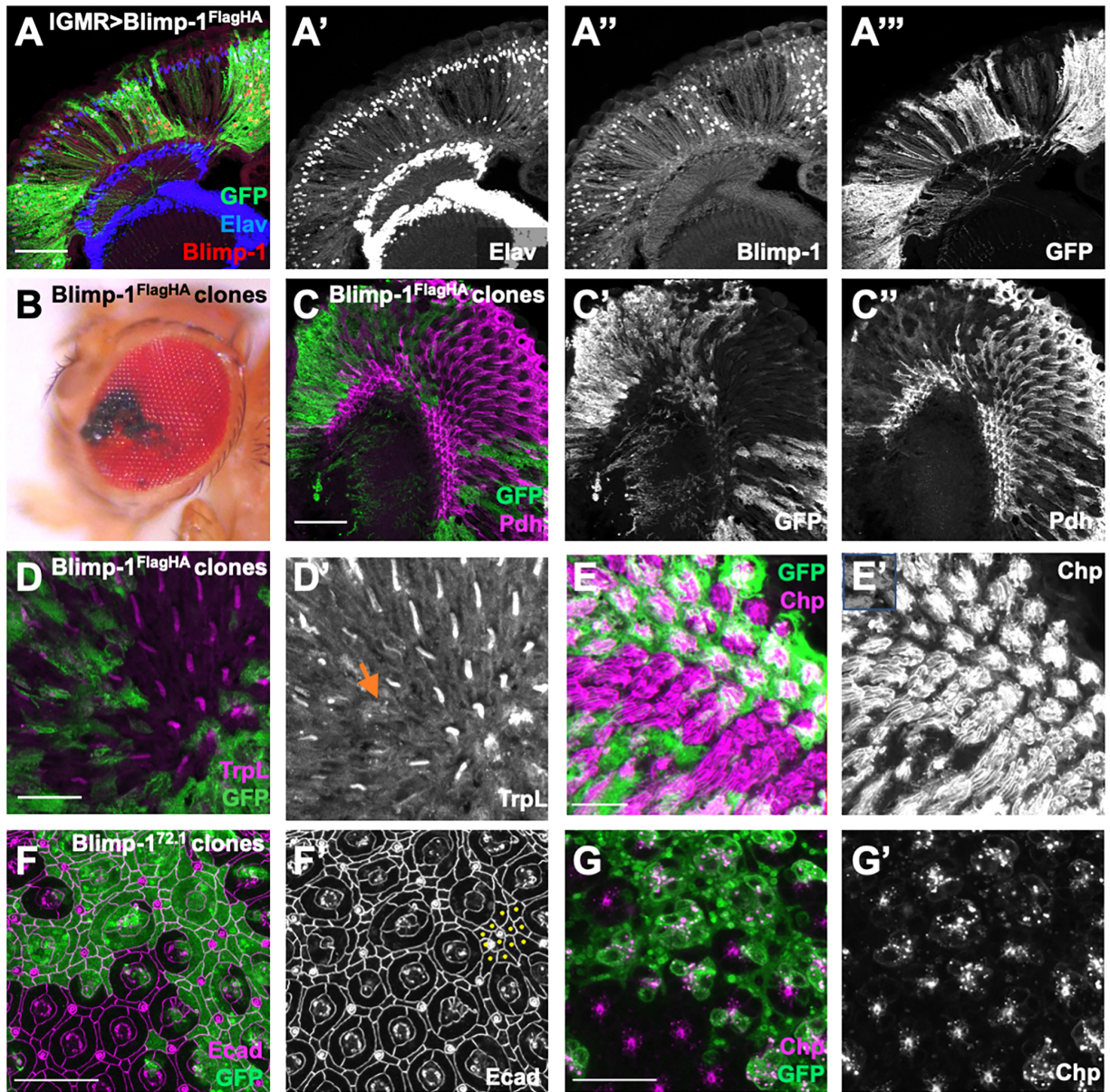


Fig. S9. *Blimp-1* overexpression disrupts photoreceptor and pigment cell morphology. (A-E) Adult eyes with clones in which *UAS-Blimp-1^{FlagHA}* and GFP (A''', C', green in A, C, D, E) are driven by *IGMR-GAL4*. (A) Horizontal section stained with anti-Blimp-1 (A'', red in A) shows that its overexpression affects the placement of photoreceptor nuclei stained with anti-Elav (A', blue in A). (B) *Blimp-1* overexpression clones display disrupted pigmentation and roughness of the external eye. (C) Tangential section showing that *Blimp-1* overexpression

reduces the expression of Pdh (C'', magenta in C) in pigment cells. (D, E) Tangential sections showing disrupted photoreceptor morphology in the overexpression clone. Rhabdomeres appear fused and show reduced TrpL (arrow in D', magenta in D) and abnormally intense Chp staining (E', magenta in E). (F, G) *Blimp-1* overexpression clones marked with GFP (green) in a 46 h APF retina. (F) shows an apical plane stained with Ecad (F', magenta) and (G) a more basal plane stained with Chp (G', magenta). *Blimp-1* overexpression increases the number of pigment cells in the lattice (marked with yellow dots in one region of F') and the intensity of Chp staining. Scale bars, 50 μ m (A, C) or 20 μ m (D-G).

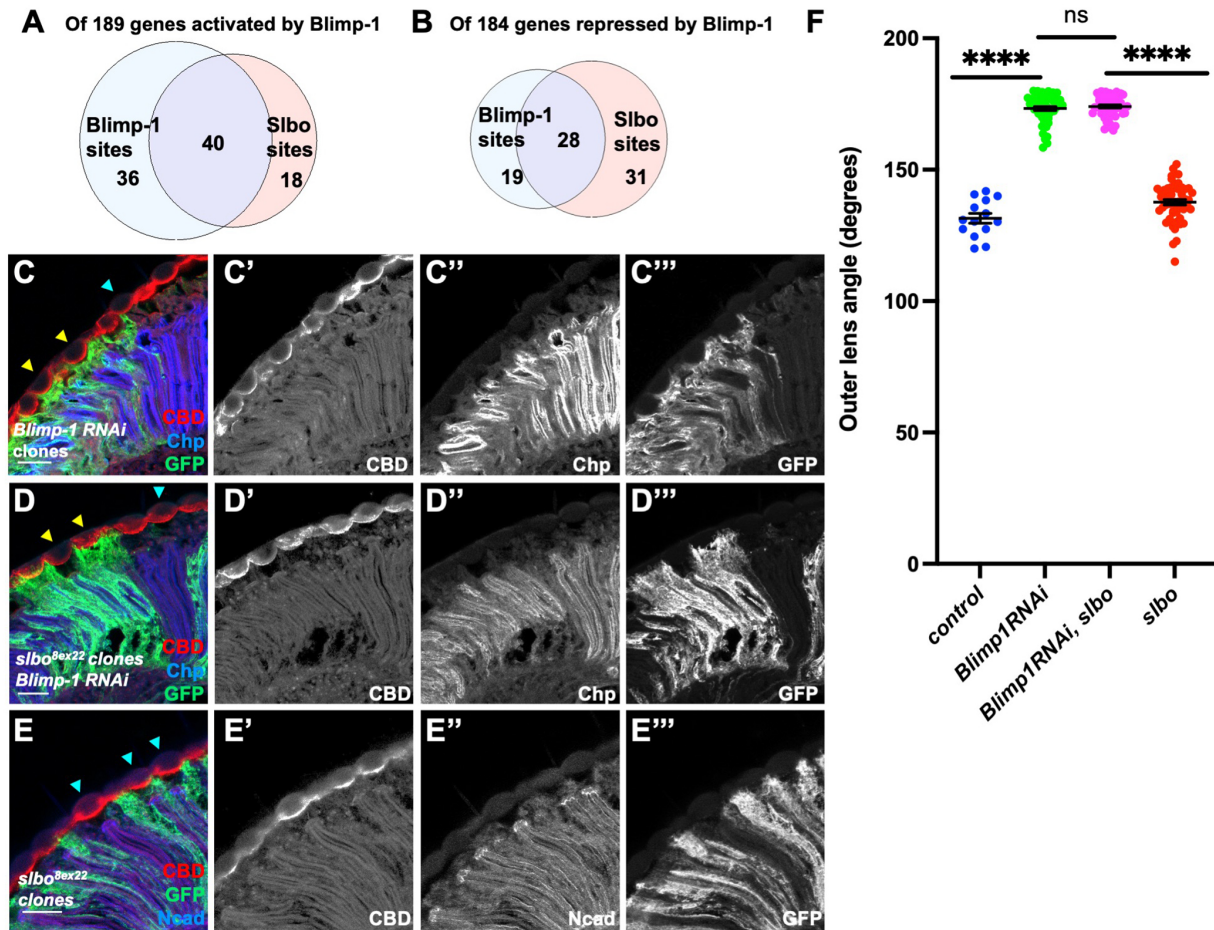


Fig. S10. Removing *slbo* is not sufficient to rescue *Blimp-1* loss of function phenotypes. (A, B) Venn diagrams showing the numbers of genes with predicted binding sites for Blimp-1 and Slbo among the genes that are down-regulated (A) or upregulated (B) by *Blimp-1* RNAi. Many *Blimp-1* regulated genes have predicted Slbo binding sites, and a significant number of genes have predicted sites for both Blimp-1 and Slbo. (C-E) Horizontal sections of adult heads stained with CBD (C'-E', red in C-E), anti-Chp (C'', D'', blue in C, D), anti-Ncad (E'', blue in E) and anti-GFP (C'''-E''', green in C-E). GFP marks clones that are expressing *Blimp-1* RNAi KK (C), *slbo*^{8ex22} mutant and expressing *Blimp-1* RNAi KK (D), or *slbo*^{8ex22} mutant (E). Scale bars, 20 μ m. (F) quantification of outer lens angles for these genotypes and for controls (*FRT42* clones). n= 14 (control), 54 (*Blimp-1* RNAi), 53 (*Blimp-1* RNAi, *slbo*) or 52 (*slbo*). ****, p<0.0001; ns, not significant by two-tailed t-test.

Table S1. Differential gene expression in 48 h APF retinas expressing Blimp-1 RNAi or *UAS-Blimp-1* with *IGMR-GAL4*.

[Click here to download Table S1](#)